Biological insights from a simulation model of the critical FtsZ accumulation required for prokaryotic cell division

Claire E. Dow[1], Hugo A. van den Berg[2], David I. Roper[3], Alison Rodger[4,5*]

[1] Molecular Organisation and Assembly in Cells Doctoral Training Centre, Senate House, University of Warwick, Coventry, CV4 7AL, United Kingdom

[2] Mathematics Institute, University of Warwick, Coventry, CV4 7AL, United Kingdom

[3] School of Life Sciences, University of Warwick, Coventry, CV4 7AL, United Kingdom

[4] Department of Chemistry, University of Warwick, Coventry, CV4 7AL, United Kingdom

[5] Warwick Analytical Science Centre, University of Warwick, Coventry, CV4 7AL, United Kingdom

[*]Corresponding author. Email: a.rodger@warwick.ac.uk

Funding support statement

This work was supported by an EPSRC-funded studentship to CD through the MOAC Doctoral Training Centre (Grant number EP/F500378/1).

Abbreviations

CAM-FF	Critical Accumulation of Membrane-bound FtsZ Fibres
ATP	Adenosine-5'-triphosphate
GDP	Guanosine-5'-diphosphtae
GMP	Guanosine-5'-monophosphtae
GTP	Guanosine-5'-triphosphtae

Running Title (50 characters incl. spaces)

CAM-FF accurately predicts cell division outcome

ABSTRACT

A simulation model of prokaryotic Z-ring assembly, based on the observed behaviour of FtsZ *in vitro* as well as on *in vivo* parameters, is used to integrate critical processes in cell division. According to the model, the cell's ability to divide depends on a "contraction parameter" (χ) that links the force of contraction to the dynamics of FtsZ. This parameter accurately predicts the outcome of division. Evaluating the GTP binding strength, the FtsZ polymerization rate, and the intrinsic GTP hydrolysis/dissociation activity, we find that inhibition of GTP-FtsZ binding is an inefficient anti-bacterial target. Furthermore, simulations indicate that the temperature sensitivity of the *ftsZ84* mutation arises from the

conversion of FtsZ to a dual-specificity NTPase. Finally, the sensitivity to temperature of the rate of ATP hydrolysis, over the critical temperature range, leads us to conclude that the *ftsZ84* mutation affects the turnover rate of the Z-ring much less strongly than previously reported.

INTRODUCTION

Cytokinesis is the final step in cell division, the process whereby the parent cell divides into two daughter cells each containing a complete copy of the genome. Although cytokinesis forms an attractive target for antibacterial drug design, success to date has been hampered by a lack of understanding of the interplay of the relevant factors. A key stage in prokaryotes is the formation of a contractile ring, composed of fibres of the cytoskeletal protein FtsZ, at the division plane.[1] This so-called Z-ring is anchored to the cytoplasmic face of the cell membrane by the direct interaction of FtsZ with the membrane-binding proteins ZipA and FtsA.[2] These proteins constitute the structural scaffold for the recruitment of various additional proteins to form the complete "divisome" complex, which includes the enzymes required for peptidoglycan synthesis and remodelling. Following assembly, the Z-ring contracts, drawing the membrane on opposite sides of the cell together. For recent reviews see Typas et al., Egan and Vollmer, and den Blaauwen.[3–5]

Despite extensive work since the discovery in 1991 that FtsZ is the major component of the contractile ring,[6] the mechanism driving the assembly and contraction of the Z-ring as well as the link between protein function and cellular phenotype remain poorly understood. Translation of the activity of FtsZ measured *in vitro* to its function *in vivo* is critical to further our understanding of cytokinesis.

We have developed a model of this key phase of cell division [7] and showed that the results are consistent with the division behaviour observed following the loss of expression of FtsA or ZipA, two components of the *Escherichia coli* divisome complex. This strongly suggests that the simulation model is a reliable tool to probe the early stages of cytokinesis which critically depend on the Z-ring and its membrane interactions. Here we explore how various perturbations of the system, such as mutations, which are represented in the model as changes of various biochemical and biophysical parameters, affect the initiation and completion of cell division. In each case, the predictions correspond with observed phenomena (up to absolute magnitudes of timescales, as will be explained further below), and can be used to evaluate which components are likely to constitute effective drug targets. We refer to our model as CAM-FF: *Critical Accumulation*

of Membrane-bound FtsZ Fibres. After summarising the key aspects of the model, we review the wild-type behaviour, which forms our reference point, followed by analysis of:

1. A reduction in the measured rate of GTP hydrolysis by:
    (a) a reduction in the intrinsic rate of GTP hydrolysis/dissociation;
    (b) a reduction in the GTP binding strength;
    (c) a reduction in the FtsZ polymerisation rate.
2. Depletion or overexpression of anchor proteins.
3. Overexpression of FtsZ.
4. The *ftsZ84* mutant that has a significantly reduced FtsZ GTPase activity, combined with the introduction of ATPase activity.

Finally, we discuss the implications of our simulations for antibacterial agents.

EXPERIMENTAL PROCEDURES

We develop and apply CAM-FF to a range of different bacteria whose cell-division phenotype has yet to be explained. CAM-FF takes as its point of departure the "Z-centric hypothesis" (*viz.*, assembly of the Z-ring and the force of its constriction originate from FtsZ) and extends earlier work by Surovtsev *et al.*[8] Key assumptions are (i) no dependence of Z-ring formation on the cyclisation of FtsZ polymers into closed rings (*cf.* Surovtsev *et al.*,[8]), (ii) the addition of the diffusion of FtsZ into the midcell region, and (iii) the interaction of FtsZ polymers with membrane-binding proteins.

The removal of FtsZ polymer cyclisation followed from our recent work to determine the persistence length of FtsZ, *i.e.* the length scale below which the polymer molecule is essentially straight, which is 1.15 ± 0.25 μm;[9] since mature *E. coli* have a circumference of approximately 2.5 μm, *in vivo* FtsZ most probably forms short linear chains rather than rings curved around the circumference of the cell.

The cell is conceptually divided into three compartments: (1) the cell caps, (2) the midcell region, and (3) the midcell membrane, as shown in Figure 1A. FtsZ molecules within the cell caps and the midcell region undergo polymerisation and GTP hydrolysis reactions, as shown in Figure 1B, and movement between these two compartments is by diffusion with rate constant k_{dif}. Movement occurs from the midcell region to the midcell membrane when FtsZ molecules bind directly to anchor proteins fixed to the membrane or by polymerisation reactions to membrane-bound FtsZ. We account for the interaction of single FtsZ polymers with multiple membrane anchor proteins as depicted in Figure 1C.

This depends on the dissociation constant of the FtsZ:anchor interaction, $\kappa = k_{bind2} / k_{bind1}$, and the density of anchor proteins on the membrane. Using the midcell membrane surface area and the number of anchor proteins available, this anchor density is expressed as a probability that a bound FtsZ monomer is adjacent to, and consequently binding to, a binding site, P_a. As polymer length increases, the number of anchor connections increases, thereby lowering the probability that the polymer will be released from the membrane. Figure 1D shows the fraction of polymers predicted to be singly-bound to the membrane and thereby susceptible to release on dissociation at the anchor site.

CAM-FF accounts for the physical forces required to deform the cell against its surface tension. We assume that the pinching tension generated on Z-ring contraction depends on: (i) the population of FtsZ polymers accumulated in the Z-ring; (ii) the number of membrane protein:FtsZ interactions; and (iii) the force of this interaction. If the calculated maximum tension of the Z-ring exceeds the tension required to oppose the surface tension at a given radius, then we assume that a "black-box" mechanism will result in contraction of the ring and thus a decrease in the Z-ring and midcell diameter with time *i.e.* cell division may proceed (this black box could be a ratchet mechanism driven by thermal fluctuations, possibly assisted by a motor component, or by a conformational change in FtsZ on GTP hydrolysis). Figure 1E summarises the key variables in the force model.

The assumptions made in CAM-FF are listed below. For any biological system that is consistent with these assumptions, the model predictions are valid. Brief assessments or justifications are provided in parentheses.

1. The rate of polymerisation of GDP-bound FtsZ is zero. (Although GDP-bound FtsZ has been shown to polymerise, the equilibrium constant is significantly lower than for GTP[10] and was assumed to equal 0 in the original Surovtsev model.[8])

2. GTP hydrolysis occurs within membrane-bound FtsZ polymers in the same way as for free polymers. (This is plausible in the absence of evidence to the contrary.)

3. The dissociation of the FtsZ polymer following GTP hydrolysis proceeds at rate k_{dis} = 0.075 s^{-1}. (The value of k_{cat} from Romberg and Mitchison of 4.5 min^{-1} leads to this value.[11])

4. All lengths of FtsZ polymer diffuse at the same rate. (Failure of this assumption to hold may account in part for the too-rapid assembly of the Z-ring that CAM-FF predicts if, in fact, longer polymers diffuse more slowly than monomers/oligomers.)

5. The number of membrane anchor proteins, *B*, amounts to 30% of the cell complement of ZipA and FtsA. (Stricker *et al.* found that at equilibrium, approximately 30% of the cell complement of ZipA was localised to the Z-ring.[12])

6. Min and nucleoid occlusion systems were functional, permitting binding of FtsZ polymers in the midcell region only. (This is valid in the wild-type scenario but may not hold in certain mutants.)

7. FtsZ polymers do not grow longer than a given length. (We verified that increasing the value of above 150 subunits does not affect the model output appreciably.)

8. The initiation threshold value α is 20,000; the wild-type contraction parameter value χ is sufficient to allow full division with the capacity to lose 15% of its value before division behaviour is affected. (The initiation threshold is set such that the maximum value of the threshold plot as shown in Figure 2, the division completion threshold, CT, is 85% of the wild-type parameter value χ.)

9. The value of χ is constant. (We consider this to be reasonable for the initial stages of division which determine the division outcome since the peak of the threshold curve is reached early in the division process (ρ = 0.833), independent of the value of the initiation threshold α.)

10. If the calculated maximum tension of the Z-ring exceeds the tension required to oppose the cell surface tension at a given radius, thermal fluctuations will result in contraction of the ring and a decrease in the Z-ring and midcell diameter with time.

RESULTS

Model overview

In essence, in CAM-FF a complex system of biochemical and biophysical interactions is captured by a single index, the *contraction parameter*, χ, which links the population of membrane-bound FtsZ molecules to the force of constriction, and which can be used to predict the cell's ability to divide. It is given by

$$\chi = \bar{i}^2 N_z, \tag{1}$$

where $\bar{i}$ is the average number of FtsZ subunits in the membrane-bound polymers and N_z is the total number of membrane-bound FtsZ polymers. The key result is that, in order to initiate contraction of the Z-ring, the value of χ must exceed the initiation threshold α which is given by

$$\alpha = \frac{\tau_0 \omega r}{F \mathrm{P_a} I_0}, \tag{2}$$

where τ_0 is the cell surface tension, ω is the width of the Z-ring, r is the radius of the Z-ring before contraction, F is proportional to the force of the interaction of FtsZ with a single membrane anchor site, $\mathrm{P_a}$ represents the surface density of the membrane-bound proteins ZipA and FtsA (*i.e.* the probability that an FtsZ subunit is adjacent to an anchor on the membrane), and I_0 is the length of one FtsZ subunit.

Following initiation, in order for the Z-ring to continue to contract, the following condition applies:

$$\chi > \alpha\rho\left(1 + \frac{2r}{\omega}\rho\sqrt{1-\rho^2}\right), \tag{3}$$

where ρ is the dimensionless ratio of the radius of the Z-ring at any time point relative to the original radius r. As contraction proceeds, ρ decreases from 1 to 0. A plot of the contraction threshold as a function of ρ is given in Figure 2. Since the contraction parameter χ must exceed the contraction threshold at all values of the radius ratio from 1 to 0 for contraction to proceed, three outcomes are possible:

(i) division proceeds to completion;

(ii) division is initiated but stalls prior to completion; and

(iii) division is not initiated.

These outcomes are indicated schematically in Figure 2. The maximum value of the threshold plot can be regarded as the *division completion threshold*. Despite a number of simplifications, CAM-FF makes accurate predictions of cell division behaviour.[7] However,

the estimates of timescales of the process, while correct in terms of relative ordering, are too short, for reasons that are discussed below. The model has been implemented in *Mathematica 8* as detailed in our previous paper.[7] In this paper we present the predicted wild-type behaviour and the predicted effects of various perturbations to key biochemical parameters and contrast those predictions with available experimental data.

Wild-type model predictions

The predicted populations of membrane-bound FtsZ at equilibrium according to CAM-FF are summarised in Table 1. The average bound polymer length ($\bar{i}$), the percentage of the FtsZ population incorporated into the Z-ring, the total number of membrane-bound FtsZ polymers (N_z), and the value of χ at equilibrium are shown, as well as the predicted division outcome. Using the wild-type parameter values as listed in Table 2, the average membrane-bound polymer length is predicted to be 14 subunits, with 28% of the cell complement of FtsZ predicted to be membrane-bound at equilibrium. This is in accordance with the values measured experimentally of 30 – 35%.[12,13]

CAM-FF predicts a significantly faster Z-ring formation time (5 s) than is observed experimentally (1 min)[14,15] which is a consequence of assuming a single diffusion constant for all lengths of FtsZ polymer and of using the rates as measured *in vitro*, without accounting for the inhibitory effect of the cell environment viscosity and crowding (see Experimental Procedures). Accounting for this effect would slow down Z-ring assembly without materially affecting the prediction of cell division outcome. Since insufficient data are currently available to constrain these processes and our main interest is in relative orderings, we retain the simplest assumptions rather than incorporating *ad hoc* adjustments, accepting an order of magnitude timescale error.

Measurement of the GTPase activity of FtsZ alone cannot predict cell division

The experimental observation that an FtsZ mutant has a reduced rate of GTP hydrolysis can be attributed to a number of different causes, including (i) a reduced rate constant of the hydrolysis/dissociation reaction, (ii) a reduced binding efficiency of GTP, or (iii) a reduced rate of FtsZ polymerisation, since the GTPase active site is formed at the interface of two FtsZ subunits within the polymer. The same net effect in the cell would be obtained with lower FtsZ or GTP concentrations. The advantage of a mathematical model such as CAM-FF is these various scenarios can be explored independently.

As summarised in Table 1, a decrease in the rate of GTP hydrolysis/dissociation (with no other concomitant changes) results in increases of the average bound-polymer length, the percentage incorporation, and the value of the contraction parameter as well as a decrease in the number of membrane-bound FtsZ polymers. An increase in the rate of GTP hydrolysis has the opposite effects. Since the initiation threshold value α is by assumption independent of the rate of GTP hydrolysis, Equation (2), CAM-FF indicates that a loss-of-GTPase-function mutation in FtsZ does not reduce the ability of the cell to initiate contraction and may even render the cell better able to divide as the equilibrium value of the contraction parameter increases. Conversely, an increase in the rate of hydrolysis reduces the ability of the cell to divide.

The above prediction is corroborated by the behaviour of curcumin (1,7-bis-(4-hydroxy-3-methoxy-phenyl)hepta-1,6-diene-3,5-dione), an antibacterial phenolic compound that is present in turmeric.[16] Curcumin's effect is to inhibit growth of *E. coli* and *Bacillus subtilis* cell cultures. Its mode of action is *via* direct binding to FtsZ and disruption of FtsZ polymerisation and bundling. The binding of curcumin results in an increase in GTP turnover and in the rate of FtsZ depolymerisation.[16] This may be due to a direct increase in the GTP hydrolysis reaction, induced by the change in FtsZ secondary structure on curcumin binding. Alternatively, the increase in GTP turnover may be due to a steric hindrance on polymer bundling (which is not explicitly represented in our model). Such a steric hindrance has the same effect as a direct increase of the GTP hydrolysis/dissociation rate in CAM-FF compared to the wild-type case, since polymer bundling has been shown to decrease the intrinsic rate of GTP hydrolysis by FtsZ.[17] An increase in the GTP hydrolysis/dissociation rate constant in CAM-FF reduces χ and inhibits cell division. Such a mechanism of increased GTP turnover may also deplete the cell's supply of GTP, which further reduces the accumulation of FtsZ polymers.

If taken to its logical extreme, the effect of an extreme reduction of the intrinsic hydrolysis rate, all else being equal, would seem to be that cell division is maximally expedited (*i.e.* maximum cell division when there is no GTPase activity). However, this overlooks the fact that reduced hydrolysis also results in the accumulation of longer polymers. Given the persistence length of FtsZ, ~1 μm,[9] such accumulation will impede cell division. Moreover, while reduced GTP hydrolysis promotes Z-ring formation, the Z-ring must depolymerise later in the cycle and a complete loss of GTPase activity would

arrest this process. It is unlikely that an extreme perturbation to the hydrolysis rate could arise without some accompanying effect on GTP binding and FtsZ polymerisation.

The analysis suggests a possible function of the FtsZ-interacting protein ZapA. It has been clear for some time that ZapA slows down GTP hydrolysis when ZapA is added to FtsZ *in vitro.*[18,19] At a mixing ratio of 4:1 ZapA:FtsZ, the GTPase actvity is reduced by ~50%.[19] However, the mechanism of slowing remains unclear. Our analysis suggests that by reducing the rate of GTP hydrolysis, ZapA promotes the formation of longer polymers and reduces the time taken for the cell to reach the critical contraction threshold, thus accelerating cell division once Z-ring formation has started.

As summarised in Table 1, either reduced GTP binding strengths or reduced FtsZ polymerisation rates lead to the formation of shorter polymers. These factors inhibit the formation of the Z-ring and reduce its contraction ability, which is similar to the effect of increasing the GTPase activity of FtsZ. Expression of the reduction of activity as a percentage of the wild-type value allows a direct comparison. Although a significant reduction to GTP binding can adversely affect cell division, CAM-FF suggests that the effect is relatively small and so competitive inhibition of GTP binding to FtsZ would be an ineffective strategy for the development of targeted antibacterial drugs (Figure 3).

The predicted modest effect of a reduction in GTP binding may explain why C8-substituted guanine, guanosine, guanosine 5'-monophosphate (GMP) and guanosine 5'-triphosphates have been found to be ineffective antibacterial agents against *E. coli*, despite the C8-substituted GTP analogues displaying strong inhibition of FtsZ polymerisation *in vitro* [20,21] by competition for the GTP binding site. It should be noted that the lack of toxicity was not due to low intracellular accumulation, nor to the absence of conversion of the analogue to the inhibitory triphosphate form.[20]

Compared with inhibition of GTP binding, reduction of FtsZ polymerisation affects the contraction parameter more strongly and so would be predicted to be a more effective approach to arrest cell division. The differential change of χ, with respect to a change in the input parameter, gives a quantitative measure of the sensitivity of the system to perturbation of a specific biochemical interaction. To express the sensitivity as a dimensionless measure, which allows direct comparison of the different input paramaters, we use a sensitivity coefficient given by $p\Delta\chi/(\chi\Delta p)$ as a relative measure, where p is the value of the parameter. For example, for the GTP-binding constant, using the value of χ obtained for the parameter values of 99% of the wild-type GTP-binding rate constant (p =

0.0099 $\mu M^{-1}s^{-1}$, χ = 91,796) and 101% of the wild-type GTP-binding rate constant (p = 0.0101 $\mu M^{-1}s^{-1}$, χ = 91,874.7) to approximate the sensitivity of the wild-type system to changes to the rate of GTP binding, the sensitivity coefficient is given by (0.01×78.7)/(91,835.9×0.0002) = 0.043. By comparison, the sensitivity coefficient for FtsZ polymerisation is 1.035 which indicates that rational drug design effort should be focussed on the FtsZ:FtsZ interaction rather than on the inhibition of GTP binding. Indeed, Duggirala *et al.* recently reported the inhibitory effect of coumarin derviatives on *B. subtilis* growth with inhibition of FtsZ polymerisation observed *in vitro*.[22] *In silico* docking studies suggested the inhibitiory effect was due to binding of courmarin to residues of the T7 loop of FtsZ. This prevented FtsZ polymerisation by targetting the C-terminal end of the molecule, rather than via competitive inhibition of GTP binding at the N-terminal domain.

Predicting the effect of anchor protein deletion

In CAM-FF it is assumed that ZipA and FtsA have equivalent effects in anchoring FtsZ to the membrane and the total number of anchor proteins is given by the parameter *B*. The experimental literature cites the number of molecules per cell for ZipA and FtsA as 1500 and 740, respectively,[23] and according to Stricker *et al.* approximately 30% of the cell complement of ZipA localises to the Z-ring *in vivo*.[12] On the assumption that 30% of the cell complement of anchor proteins is located at the midcell, the wild-type value of *B* we have used is 672.

The effect of removing the contribution from either ZipA or FtsA (mimicking a deletion mutant) is summarised in Table 1. Upon deletion of ZipA, P_a is reduced by 67% corresponding to a total number of anchor proteins of 740 (FtsA only), with 30% located on the midcell membrane to give the number of membrane anchor proteins B = 222. The consequence is that the initiation threshold increases substantially so cells are predicted to be unable to initiate contraction in the absence of ZipA. This prediction is corroborated by the experimental observation that ZipA is essential for cell division to occur, even though the Z-ring does form in the absence of ZipA.[24] Thus, CAM-FF accurately predicts the outcome of ZipA depletion.

The lack of division of a ZipA-deletion mutant might suggest ZipA as an antibiotic target. However, the development of small molecule inhibitors has met with limited success. Targeting protein-protein interactions with small molecules remains a challenge due to the relatively large interaction area of the ZipA-FtsZ protein surfaces.[25] Inhibitors

discovered by screening [26] and computational methods [27] often have affinities that are too low for therapeutic use but provide lead compounds for development. Figure 4 shows the equilibrium value of the contraction parameter for reductions of the number of ZipA available for FtsZ-membrane anchoring. Between approximately 5% and 85% of the wild-type level of ZipA availability, cells are able to initiate division but contraction will stall prior to completion. Conversely, for an increase in the expression of ZipA, the average membrane-bound polymer length is fairly stable, whereas the percentage incorporation increases, as does the number of membrane-bound FtsZ polymers, and so cell division is facilitated. The sensitivity coefficient for the effect of the number of ZipA binding sites available on the value of the contraction parameter χ is 0.204.

Upon deletion of less abundant FtsA, P_a reduces by 33% (corresponding to a total number of anchor proteins of 1500). CAM-FF predicts that χ reaches the initiation threshold but that contraction stalls prior to completion. This is consistent with observations that FtsA-depleted cells exhibit indentations above the Z-ring, indicating that contraction is initiated, but division does not occur[24]. ZipA-depleted cells (discussed above), by contrast, appear completely smooth[24], indicating that contraction is not even being initiated.

Overexpression of FtsZ

If FtsZ is overexpressed, CAM-FF predicts increases of the average bound-polymer length and the percentage incorporation of FtsZ into the Z-ring, but a decrease in the number of bound FtsZ polymers. The χ-value indicates that the cells are better able to divide compared to the wild-type. However, FtsZ overexpression also affects assumption 6 (the confinement of membrane-bound FtsZ polymers to the midcell by the Min system – see Experimental Procedures) which is no longer valid: membrane-bound FtsZ will also be found at the cell poles. For example, at 2.7-fold over-expression of FtsZ in *E. coli*, the "minicell phenotype" is induced, in which divisions occur at the cell poles, in addition to the normal midcell divisions. As a closely similar phenotype follows deletion of the Min operon, it appears reasonable to suppose that control by the Min system is overwhelmed at increased concentrations of FtsZ. Furthermore, since the function of MinC is to antagonise the polymerisation activity of FtsZ,[28] the phenotype observed on loss of the intrinsic GTPase activity in FtsZ, which promotes polymerisation, somewhat resembles the loss of the Min system. In FtsZ over-expression studies, it was found that once the concentration

of FtsZ reaches twelve times the wild-type value, all divisions are inhibited and cells become filamentous.[29]

The predicted average membrane-bound polymer length of 36 subunits for 3-fold FtsZ over-expression corresponds to an average polymer length of ~0.14 μm which is of the order of the cell radius. In view of the persistence length of FtsZ,[9] such long polymers are not anticipated to occur in *E. coli* as they would not bend to form the Z-ring. The behaviour of FtsZ when assumption 6 breaks down has not yet been built into the model.

Temperature-sensitivity of the *ftsZ84* mutation

The GTPase activity of the FtsZ84 (FtsZ-G105S) mutant protein is approximately one-tenth of the wild-type protein, due to its strongly reduced affinity for GTP.[30] So far it has not been clear why cells bearing the *ftsZ84* mutation appear to divide normally at 30°C but are unable to divide at 42°C, particularly since the GTPase activity appears to be temperature-insensitive over this range.[30,31] Translation of the activity of the FtsZ84 protein measured *in vitro* into CAM-FF parameters allows us to explore the biochemical mechanism underlying this temperature sensitivity.

According to RayChaudhuri and Park, the FtsZ84 mutant protein also catalyses the hydrolysis of ATP, a function not present in the wild-type protein.[31] Filter retention assays with radio-labelled nucleotides showed that the binding affinity of the mutant protein for ATP is approximately 30 times lower than the affinity of the wild-type protein for GTP.[31] The concentration of nucleotides within the cell is known to vary with growth conditions,[32,33] but according to Bennett *et al.*, in *E. coli* the concentration of ATP is approximately twice that of GTP and the concentrations of ADP and GDP are approximately equal.[34] At 42°C the mutant has a similar level of ATPase and GTPase activity whereas at 30°C the ATPase activity is a third of that of the GTPase.[31]

To model the behaviour of *ftsZ84*, we applied a 30-fold reduction in the rate of nucleotide triphosphate (NTP) binding, as well as a range of different increases in the concentration of the pool of activating nucleotides (since the measured concentrations of ATP vary), as indicated in Table 1, and different ranges of NTPase rates of the FtsZ84 protein to account for changes in the ATPase activity as a function of temperature. We assumed that the binding affinities and rates of polymerisation of FtsZ84 are equal for the ATP- and GTP-bound proteins and not temperature-sensitive. These assumptions imply that the proportion of active sites in the ATP- and GTP-bound states correspond to the

relative concentrations of ATP and GTP in the nucleotide pool. In view of the linearity of the rate terms in the kinetic equations, we can use a weighted average of the hydrolysis/dissociation rate constants as the effective rate constant $k_{\mathrm{dis\_eff}}$, based on the relative concentrations of the two activating nucleotides. For example, with an ATP:GTP ratio of 2:1 and a 2-fold reduction to the rate of ATP hydrolysis, the effective NTPase rate is 0.05 s^{-1} ((2/3) × 0.0375 + (1/3) × 0.075 s^{-1}).

Thus, as summarised in Table 1 and shown in Figure 5, at 42°C we predict a reduction in the average length of the membrane-bound FtsZ polymers. This in turn results in a dramatic lowering of χ. The percentage of FtsZ that is membrane-bound is also reduced. CAM-FF therefore predicts that cell division is initiated but stalls prior to completion at 42°C. However, for the lower efficiency of the ATPase activity at 30°C, χ increases above the completion threshold in all ATP:GTP ratios but with a 3-fold reduction in activity relative to the wild-type.

In sum, CAM-FF predicts that cell division occurs at lower temperatures due to the reduction in the ATPase activity of the mutant FtsZ84 protein. The precise point at which the division thresholds are no longer reached depends on the relative concentrations of nucleotides and the true intrinsic rates of hydrolysis/dissociation. The solutions shown in Figure 5 are based on current experimental estimates of the parameters and it is hoped representative of a biologically relevant scenario. CAM-FF also predicts that the introduction of a second mutation into the *ftsZ84* gene that reduces the intrinsic rate of hydrolysis, such as “T7 synergy loop” mutations, would restore cell division behaviour at the currently non-permissive temperature.

Furthermore, CAM-FF predicts that an increase in the concentration of FtsZ would restore cell division. Indeed, it has been shown that the introduction, at low copy numbers, of a plasmid containing the *ftsQ*, *ftsA*, and *ftsZ84* genes leads to recovery of cell division in *ftsZ84* cells but the introduction of the same plasmid with *ftsQ* and *ftsA* only did not restore division.[35] These findings suggest that the recovery effect is due to increased levels of the FtsZ84 protein.

In summary, CAM-FF predicts that the average bound polymer length is 24 subunits for a 2-fold increase in FtsZ84 concentration and 80 subunits for a 3-fold increase. However, as was the case for wild-type FtsZ overexpression, excess expression of FtsZ threatens to invalidate a key assumption of CAM-FF. The possible breakdown of assumption 6 ties in with the experiemental observation that introduction of a high copy

number plasmid to *ftsZ84* cells results in the inhibition of cell division as the Min and nucleoid occlusion systems are overwhelmed and membrane-binding is no longer restricted to the midcell.[35]

Division activity in *ftsZ84* is restored by increased gene dosage of ZipA at the non-permissive temperature,[36] in agreement with the simulation results summarised in Table 1. An increase in the number of membrane anchor proteins decreases the threshold value α and has a small effect on χ. With the value of the wild-type threshold α as above and the number of ZipA molecules per cell increased 3-fold, CAM-FF predicts that the completion threshold is reached and the cell is able to initiate division.

The effect of the *ftsZ84* mutation on Z-ring turnover is less pronounced than previously measured

Two key parameters in CAM-FF are the rate constants for membrane association (k_{bind1}) and dissociation (k_{bind2}) of FtsZ. Since these values are not available, we estimated them from the equilibrium binding constant for the FtsZ-ZipA interaction ($\kappa = 2$ μM)[10] and measurements of the half-life of fluorescence recovery (30 s)[12] when membrane-bound FtsZ-GFP is photobleached. The observed off-rate in the FRAP experiment corresponds to k_{bind2} multiplied by $p_1(\bar{i})$, the fraction of polymers in the singly-bound state (p_1) for the average polymer length at equilibrium $(\bar{i})$. Figure 1D shows how the fraction of polymers in the singly-bound state decreases for longer polymers (since more FtsZ:anchor interactions retain the FtsZ polymer at the membrane). Cell conditions that increase the average polymer length lead to a decrease in $p_1(\bar{i})$ and therefore lower the rate of release from the membrane, and increase the fluorescence recovery time as k_{bind2} is constant. It is therefore predicted that a decrease in the intrinsic rate of GTP hydrolysis, which increases the average polymer length, will lead to an increase in the half-life of recovery.

On the assumption that the constants determined from WT data apply to the *ftsZ84* mutant, CAM-FF predicts only a minor increase in the half life of recovery for the *ftsZ84* mutant at the permissive temperature: 30 seconds for an ATP:GTP ratio of 2:1, 32 seconds for a ratio of 3:1 and 33 seconds for a ratio of 4:1. This is in contrast to the large increase observed by Stricker *et al.* and Anderson *et al.*[12,13] A minor increase in the percentage incorporation of FtsZ into the ring is also observed. However, this increase is considerably smaller than the values of up to ~65% that were reported by Stricker *et al.*[12]

This discrepancy could be due to the fact that different growth conditions were used in their experiments, which affects the values of the rates of NTP hydrolysis as well as the concentrations of available nucleotides and of FtsZ.[33]

DISCUSSION

A simulation model of cytokinesis that includes kinetics and mid-cell membrane binding and contraction allows us to generate predictions of the *in vivo* properties of the Z-ring such as the average bound-polymer length, the percentage of FtsZ incorporation into the Z-ring, and whether a cell will initiate and/or complete cytokinesis. Our predictions accord well with experimental data, leading us to believe that the model, *Critical Accumulation of Membrane-bound FtsZ Fibres* (CAM-FF), adequately captures the dynamics of the processes occurring *in vivo*. The key output of CAM-FF is the contraction parameter χ which links the force of Z-ring contraction to the dynamics of the intracellular population of membrane-bound FtsZ. This χ-value is to be compared to threshold values for initiation and completion to predict a cell division outcome. Interrogation of CAM-FF yields insights in the underlying mechanistic basis for observed behaviours. In the case of the *ftsZ84* mutation, model analysis suggests that the loss of division behaviour at 42°C is due to the ATPase activity acquired by the mutant FtsZ protein which increases the concentration of the pool of activating nucleotides (GTP and ATP). However, at lower temperatures where the ATPase activity is reduced, a functional Z-ring is able to form and contract. Moreover, the low turnover rate observed for the FtsZ84-ring *in vivo* may reflect changes in experimental conditions rather than be a true effect of the mutation.

While the explanation of the temperature-sensitivity of the *ftsZ84* mutant addresses some of the questions around cell division and cell behaviour observed in the laboratory, the key goal of our model is to understand bacterial cell division sufficiently well to determine which components pose the most effective targets for anti-bacterial agents. Our analysis suggests that targeting the binding of GTP to FtsZ using a competitive inhibitor is an inefficient method of blocking cell division. By contrast, targeting the polymerisation of FtsZ or the availability of ZipA or FtsA binding sites were shown to be considerably more effective. In sum, CAM-FF predicts that the order of efficiency of the possible drug targets as follows: FtsZ polymerisation > ZipA/FtsA availability > GTP-binding.

The model predicts which of three division outcomes prevails as a function of parameter values. In those cases where the model predicts that division can initiate but not

complete, the filamentous phenotype is observed in the laboratory. The predicted cell phenotype is an important consideration in antibiotic development. Whereas induction of the filamentous phenotype leads to cell lysis following treatment with β-lactam antibiotics such as cephalexin,[37,38] induction of the filamentous phenotype has also been shown to inhibit phagocytosis by macrophages, where access to the filament pole was a crucial factor.[39] Furthermore, the filamentation process is thought to contribute to bacterial virulence in infections of *Legionella pneumophilia* (legionnaires' disease),[39] *E. coli* (urinary tract infection),[40] and *Salmonella* (food poisoning).[37] The possibility of inducing dormant states such as those found in *Mycobacterium tuberculosis* infection, in which the organism survives in filamentous form within macrophages [41] may constitute a form of evasion of host defenses. Moreover, pools of dormant filamentous cells may reinitiate division upon removal of the antibiotic. This has been described as a "negative post-antibiotic effect", where the rate of growth of the bacteria is rapid after the removal of an antibiotic as the filamentous cells simultaneously divide.[42] Indirect evidence for this hypothesis is provided by the phenomenon of a resurgence of urinary tract infection following withdrawal of antibiotics.[40]

The CAM-FF model makes no assumptions about the molecular mechanism of Z-ring contraction and requires only that *some* minimal force is required for contraction, perhaps generated by a conformational switch in FtsZ itself on GTP hydrolysis,[43–45] which depends on the interaction of FtsZ polymers with the membrane, where the pulling force on the membrane is considered to be proportional to the number of membrane interactions. To our knowledge, no motor protein has yet been found to associate with FtsZ and it is conceivable that contraction might proceed without the intervention of such a motor, by means of a non-equilibrium process involving the continual binding and release of FtsZ polymers, dependent on the rate of GTP-hydrolysis. The release and rebinding of FtsZ polymers in the Z-ring would effectively create a ratchet mechanism whereby local fluctuations become locked in place by the adjacent binding of further FtsZ polymers. Multiple membrane anchors may play a role in the ratchet, *e.g.* ZipA is tightly anchored within the membrane whereas FtsA is more weakly bound and so is readily released and rebound during thermal fluctuations of the Z-ring or of the cell membrane. Interestingly, FtsA is an ATPase [46] which suggests a possible means of chemical coupling to drive unidirectional contraction. The state of the bound nucleotide may affect the interaction of FtsA with FtsZ or the cell membrane or both.

An additional role of the Z-ring that is not included in the model is the recruitment of peptidoglycan remodeling enzymes on the outside of the inner cell membrane.[47] As the Z-ring contracts, the peptidoglycan remodeling process creates a physical barrier to any subsequent re-expansion of the Z-ring which consolidates the progress made thus far and acts as another ratchet. The contribution of the cell wall to division will be considered in future modeling studies. Furthermore, as described in assumption 6 in Experimental Procedures, in CAM-FF the Min and nucleoid occlusions systems are captured in a simplified form by permitting binding of FtsZ to the ZipA/FtsA at the midcell only. This assumption limits CAM-FF to consideration of the effectiveness of inhibitors of the system such as inhibition of GTP-binding and FtsZ polymerisation, and activation of the GTPase activity of FtsZ. For factors that promote FtsZ polymerisation, CAM-FF requires extension to include the factors that validate assumption 6. For example, the antibacterial benzamide PC190723 has been reported as a promoter of FtsZ polymerisation in *Staphylococcus aureus* [48–50] and mulitple FtsZ rings and arcs are observed in PC190723-treated Methicillin-Resistent *S. aureus.*[51] While CAM-FF in its current form provides insight into various inhibitors of polymerisation, those factors which promote polymerisation require explicit consideration of the Min and nucleoid occlusion systems.

In conclusion, although certain aspects of the biological process have been simplified in our model and the molecular mechanism of the contraction process remains to be elucidated, analysis of the contraction parameter already allows us to make organism-level predictions based on the biochemical activity of FtsZ measured *in vitro*. The model simulations present a relatively cost-effective way of generating novel biological ideas, *e.g.* the biochemical mechanism of temperature sensitivity of *ftsZ84*. This is particularly important for FtsZ since specific small molecule inhibitors, commonplace in the laboratory for the study of the structural FtsZ homolgue tubulin, are absent. This lack limits the study of the effect of loss of a particular function of FtsZ experimentally. The search for potential drug interactions may be aided by evaluation of target efficacy *in silico*.

REFERENCES

1. Bramhill, D. (1997) Bacterial cell division. *Annu. Rev. Cell Dev. Biol.* 13, 395–424.

2. Pichoff, S. and Lutkenhaus, J. (2005) Tethering the Z ring to the membrane through a conserved membrane targeting sequence in FtsA. *Mol. Microbiol.* 55, 1722–1734.

3. Typas, A., Banzhaf, M., Gross, C. A. and Vollmer, W. (2011) From the regulation of peptidoglycan synthesis to bacterial growth and morphology. *Nat. Rev. Microbiol.* 10, 123–136.

4. Egan, A. J. F. and Vollmer, W. (2013) The physiology of bacterial cell division. *Ann. N. Y. Acad. Sci.* 1277, 8–28.

5. Den Blaauwen, T. (2013) Prokaryotic cell division: Flexible and diverse. *Curr. Opin. Microbiol.* 16, 738–744.

6. Bi, E. F. and Lutkenhaus, J. (1991) FtsZ ring structure associated with division in Escherichia coli. *Nature* 354, 161–164.

7. Dow, C. E., Rodger, A., Roper, D. I. and van den Berg, H. A. (2013) A model of membrane contraction predicting initiation and completion of bacterial cell division. *Integr. Biol. (Camb).* 5, 778–795.

8. Surovtsev, I. V., Morgan, J. J. and Lindahl, P. a. (2008) Kinetic modeling of the assembly, dynamic steady state, and contraction of the FtsZ ring in prokaryotic cytokinesis. *PLoS Comput. Biol.* 4, e1000102.

9. Turner, D. J., Portman, I., Dafforn, T. R., Rodger, A., Roper, D. I., Smith, C. J. et al. (2012) The mechanics of FtsZ fibers. *Biophys. J.* 102, 731–738.

10. Haney, S. a., Glasfeld, E., Hale, C., Keeney, D., He, Z. and De Boer, P. (2001) Genetic analysis of the Escherichia coli FtsZ-ZipA interaction in the yeast two-hybrid system. Characterization of FtsZ residues essential for the interactions with ZipA and with FtsA. *J. Biol. Chem.* 276, 11980–11987.

11. Romberg, L. and Mitchison, T. J. (2004) Rate-limiting guanosine 5'-triphosphate hydrolysis during nucleotide turnover by FtsZ, a prokaryotic tubulin homologue involved in bacterial cell division. *Biochemistry* 43, 282–288.

12. Stricker, J., Maddox, P., Salmon, E. D. and Erickson, H. P. (2002) Rapid assembly dynamics of the Escherichia coli FtsZ-ring demonstrated by fluorescence recovery after photobleaching. *Proc. Natl. Acad. Sci. U. S. A.* 99, 3171–3175.

13. Anderson, D. E., Gueiros-Filho, F. J. and Erickson, H. P. (2004) Assembly dynamics of FtsZ rings in Bacillus subtilis and Escherichia coli and effects of FtsZ-regulating proteins. *J. Bacteriol.* 186, 5775–5781.

14. Sun, Q. and Margolin, W. (1998) FtsZ dynamics during the division cycle of live Escherichia coli cells. *J. Bacteriol.* 180, 2050–2056.

15. Blaauwen, T. Den, Buddelmeijer, N., Aarsman, M. E. G., Hameete, C. M. and Nanninga, N. (1999) Timing of FtsZ assembly in Escherichia coli. *J. Bacteriol.* 181, 5167–5175.

16. Rai, D., Singh, J. K., Roy, N. and Panda, D. (2008) Curcumin inhibits FtsZ assembly: an attractive mechanism for its antibacterial activity. *Biochem. J.* 410, 147–155.

17. Marrington, R., Small, E., Rodger, A., Dafforn, T. R. and Addinall, S. G. (2004) FtsZ fiber bundling is triggered by a conformational change in bound GTP. *J. Biol. Chem.* 279, 48821–48829.

18. Small, E., Marrington, R., Rodger, A., Scott, D. J., Sloan, K., Roper, D. et al. (2007) FtsZ Polymer-bundling by the Escherichia coli ZapA Orthologue, YgfE, Involves a Conformational Change in Bound GTP. *J. Mol. Biol.* 369, 210–221.

19. Pacheco-Gómez, R., Cheng, X., Hicks, M., Smith, C., Roper, D., Addinall, S. et al. (2013) Tetramerisation of ZapA is required for FtsZ bundling. *Biochem. J.* 449, 795–802.

20. Läppchen, T. (2007) Synthesis of GTP analogues and evaluation of their effect on the antibiotic target FtsZ and its eukaryotic homologue tubulin. University of Amsterdam. p. 121–151.

21. Marcelo, F., Huecas, S., Ruiz-Ávila, L. B., Cañada, F. J., Perona, A., Poveda, A. et al. (2013) Interactions of Bacterial Cell Division Protein FtsZ with C8-Substituted Guanine Nucleotide Inhibitors. A Combined NMR, Biochemical and Molecular Modeling Perspective. *J. Am. Chem. Soc.* American Chemical Society. 135, 16418–16428.

22. Duggirala, S., Nankar, R. P., Rajendran, S. and Doble, M. (2014) Phytochemicals as inhibitors of bacterial cell division protein FtsZ: Coumarins are promising candidates. *Appl. Biochem. Biotechnol.* 174, 283–296.

23. Rueda, S., Vicente, M. and Mingorance, J. (2003) Concentration and assembly of the division ring proteins FtsZ, FtsA, and ZipA during the Escherichia coli cell cycle. *J. Bacteriol.* 185, 3344–3351.

24. Hale, C. a. and De Boer, P. a J. (1999) Recruitment of ZipA to the septal ring of Escherichia coli is dependent on FtsZ and independent of FtsA. *J. Bacteriol.* 181, 167–176.

25. Fry, D. C. (2006) Protein-protein interactions as targets for small molecule drug discovery. *Biopolymers* 84, 535–552.

26. Tsao, D., Sutherland, A. G., Jennings, L., Rush, T. I., Alvarez, J., Ding, W. et al. (2006) Discovery of novel inhibitors of the ZipA/FtsZ complex by NMR fragment screening coupled with structure-based design. *Bioorganic Med. Chem.* 14, 7953–7961.

27. Rush, T. S., Grant, J. A., Mosyak, L. and Nicholls, A. (2005) A shape-based 3-D scaffold hopping method and its application to a bacterial protein-protein interaction. *J. Med. Chem.* 48, 1489–1495.

28. Hu, Z., Mukherjee, A., Pichoff, S. and Lutkenhaus, J. (1999) The MinC component of the division site selection system in Escherichia coli interacts with FtsZ to prevent polymerization. *Proc. Natl. Acad. Sci. U. S. A.* 96, 14819–14824.

29. Ward, J. E. and Lutkenhaus, J. (1985) Overproduction of FtsZ induces minicell formation in E. coli. *Cell* 42, 941–949.

30. RayChaudhuri, D. and Park, J. T. (1992) Escherichia coli cell-division gene ftsZ encodes a novel GTP-binding protein. *Nature* 359, 251–254.

31. RayChaudhuri, D. and Park, J. T. (1994) A point mutation converts Escherichia coli FtsZ septation GTPase to an ATPase. *J. Biol. Chem.* 269, 22941–22944.

32. Bagnara, A. and Finch, L. (1973) Relationships between intracellular contents of nucleotides and 5-phosphoribosyl 1-pyrophosphate in Escherichia coli. *Eur. J. Biochem.* 36, 422–427.

33. Gaal, T., Bartlett, M. S., Ross, W., Turnbough, C. L. and Gourse, R. L. (1997) Transcription regulation by initiating NTP concentration: rRNA synthesis in bacteria. *Science* 278, 2092–2097.

34. Bennett, B. D., Kimball, E. H., Gao, M., Osterhout, R., Van Dien, S. J. and Rabinowitz, J. D. (2009) Absolute metabolite concentrations and implied enzyme active site occupancy in Escherichia coli. *Nat. Chem. Biol.* 5, 593–599.

35. Phoenix, P. and Drapeau, G. (1988) Cell division control in Escherichia coli K-12: Some properties of the ftsZ84 mutations and suppression of this mutation by the product of a newly identified gene. *J. Bacteriol.* 170, 4338–4342.

36. RayChaudhuri, D. (1999) ZipA is a MAP-Tau homolog and is essential for structural integrity of the cytokinetic FtsZ ring during bacterial cell division. *EMBO J.* 18, 2372–2383.

37. Chung, H. S., Yao, Z., Goehring, N. W., Kishony, R., Beckwith, J. and Kahne, D. (2009) Rapid beta-lactam-induced lysis requires successful assembly of the cell division machinery. *Proc. Natl. Acad. Sci. U. S. A.* 106, 21872–21877.

38. Kohanski, M. A., Dwyer, D. J. and Collins, J. J. (2010) How antibiotics kill bacteria: from targets to networks. *Nat. Rev. Microbiol.* 8, 423–435.

39. Möller, J., Luehmann, T., Hall, H. and Vogel, V. (2012) The race to the pole: How high-aspect ratio shape and heterogeneous environments limit phagocytosis of filamentous Escherichia coli bacteria by macrophages. *Nano Lett.* 12, 2901–2905.

40. Justice, S. S., Hunstad, D. A., Seed, P. C. and Hultgren, S. J. (2006) Filamentation by Escherichia coli subverts innate defenses during urinary tract infection. *Proc. Natl. Acad. Sci. U. S. A.* 103, 19884–19889.

41. Gengenbacher, M. and Kaufmann, S. H. E. (2012) Mycobacterium tuberculosis: Success through dormancy. *FEMS Microbiol. Rev.* 36, 514–532.

42. MacKenzie, F. and Gould, I. (1993) The post-antibiotic effect. *J. Antimicrob. Chemother.* 32, 519–537.

43. Lu, C. and Erickson, H. (1999) The straight and curved conformation of FtsZ protofilaments-evidence for rapid exchange of GTP into the curved protofilament. *Cell Struct. Funct.* 24, 285–290.

44. Lu, C., Reedy, M. and Erickson, H. P. (2000) Straight and curved conformations of FtsZ are regulated by GTP hydrolysis. *J. Bacteriol.* 182, 164–170.

45. Li, Y., Hsin, J., Zhao, L., Cheng, Y., Shang, W., Huang, K. C. et al. (2013) FtsZ protofilaments use a hinge-opening mechanism for constrictive force generation. *Science* 341, 392–395.

46. Feucht, A., Lucet, I., Yudkin, M. D. and Errington, J. (2001) Cytological and biochemical characterization of the FtsA cell division protein of Bacillus subtilis. *Mol. Microbiol.* 40, 115–125.

47. De Boer, P. A. (2010) Advances in understanding E. coli cell fission. *Curr. Opin. Microbiol.* 13, 730–737.

48. Haydon, D. J., Stokes, N. R., Ure, R., Galbraith, G., Bennett, J. M., Brown, D. R. et al. (2008) An inhibitor of FtsZ with potent and selective anti-staphylococcal activity. *Science* 321, 1673–1675.

49. Andreu, J. M., Schaffner-Barbero, C., Huecas, S., Alonso, D., Lopez-Rodriguez, M. L., Ruiz-Avila, L. B. et al. (2010) The antibacterial cell division inhibitor PC190723 is an FtsZ polymer-stabilizing agent that induces filament assembly and condensation. *J. Biol. Chem.* 285, 14239–14246.

50. Elsen, N. L., Lu, J., Parthasarathy, G., Reid, J. C., Sharma, S., Soisson, S. M. et al. (2012) Mechanism of action of the cell-division inhibitor PC190723: Modulation of FtsZ assembly cooperativity. *J. Am. Chem. Soc.* 134, 12342–12345.

51. Tan, C. M., Therien, A. G., Lu, J., Lee, S. H., Caron, A., Gill, C. J. et al. (2012) Restoring methicillin-resistant Staphylococcus aureus susceptibility to β-lactam antibiotics. *Sci. Transl. Med.* 4, 126ra35.

52. Mukherjee, A., Dai, K. and Lutkenhaus, J. (1993) Escherichia coli cell division protein FtsZ is a guanine nucleotide binding protein. *Proc Natl Acad Sci U S A* 90, 1053–1057.

53. Chen, Y., Bjornson, K., Redick, S. and Erickson, H. (2005) A rapid fluorescence assay for FtsZ assembly indicates cooperative assembly with a dimer nucleus. *Biophys. J.* 88, 505–514.

54. Culbertson, C. T., Jacobson, S. C. and Michael Ramsey, J. (2002) Diffusion coefficient measurements in microfluidic devices. *Talanta* 56, 365–373.

Table 1: Model predictions for different cell characteristics at kinetic equilibrium. Unless stated otherwise, all input parameter values are as shown in Table 2. The wild-type input parameter values were used to set the initiation threshold value α to 20,000. $\bar{i}$: the average length of membrane-bound FtsZ polymers, %: the percentage of FtsZ that is membrane-bound, N_Z : the number of membrane-bound FtsZ polymers, χ: the contraction parameter, α: the initiation threshold, CT: the completion threshold.

Parameter	$\bar{i}$	%	N_Z	χ	α	CT	Division Outcome
Wild type	14	28	504	91,836	20,000	78,086	Complete
GTP hydrolysis: WT $k_{\mathrm{dis}} = 0.075$ s^{-1}							
0.06 (80%)	15	30	485	112,470	20,000	78,086	Complete
0.053 (70%)	16	31	475	125,010	20,000	78,086	Complete
0.045 (60%)	18	33	461	142,634	20,000	78,086	Complete
0.038 (50%)	19	34	448	161,989	20,000	78,086	Complete
0.09 (120%)	12	26	519	76,877	20,000	78,086	Initiation only
0.105 (140%)	11	24	531	65,671	20,000	78,086	Initiation only
0.12 (160%)	10	22	542	56,756	20,000	78,086	Initiation only
0.135 (180%)	9	21	551	49,717	20,000	78,086	Initiation only
0.15 (200%)	9	20	559	43,987	20,000	78,086	Initiation only
GTP binding: WT $k_{\mathrm{ex1}} = 0.01$ μM^{-1}s^{-1}							
0.008 (80%)	13	27	505	90,773	20,000	78,086	Complete
0.006 (60%)	13	27	507	88,642	20,000	78,086	Complete
0.005 (50%)	13	27	509	86,634	20,000	78,086	Complete
0.004 (40%)	13	26	513	83,199	20,000	78,086	Complete
0.003 (30%)	12	26	520	76,753	20,000	78,086	Initiation only
0.002 (20%)	11	24	534	63,432	20,000	78,086	Initiation only
0.001 (10%)	8	18	572	34,802	20,000	78,086	Initiation only
FtsZ polymerisation: WT $k_{\mathrm{dim1}} = k_{\mathrm{el1}} = k_{\mathrm{an}} = 4$ μM^{-1}s^{-1}							
3 (75%)	11	24	528	67,721	20,000	78,086	Initiation only
2 (50%)	9	20	559	43,097	20,000	78,086	Initiation only
1 (25%)	6	14	603	18,867	20,000	78,086	No initiation
Anchor deletion:							
ZipA: $B = 222,\ \mathrm{P_a} = 0.014$	15	12	504	46,978	61,429	239,836	No initiation
FtsA: $B = 450,\ \mathrm{P_a} = 0.029$	14	21	365	76,045	29,665	115,821	Initiation only
FtsZ overexpression - wild-type:							
[FtsZ] = 24 μM (200%)	27	42	386	277,974	20,000	78,086	Complete
[FtsZ] = 36 μM (300%)	36	48	328	425,000	20,000	78,086	Complete
ZipA overexpression - wild-type:							
$B = 1122,\ \mathrm{P_a} = 0.072$ (200%)	12	35	741	103,349	11,944	46,633	Complete
$B = 1572,\ \mathrm{P_a} = 0.101$ (300%)	10	39	968	96,267	8,515	33,245	Complete

The *ftsZ84* mutation: $k_{ex1} = 3 \times 10^{-4}$ μM^{-1}s^{-1}							
ATP:GTP ratio = 2:1, [NTP] = 270 μM, [NDP] = 20 μM							
$k_{dis\_eff} = 0.075$ s^{-1}	7	16	584	27,328	20,000	78,086	Initiation only
$k_{dis\_eff} = 0.05$ s^{-1}	11	24	532	65,672	20,000	78,086	Initiation only
$k_{dis\_eff} = 0.042$ s^{-1}	13	27	509	88,161	20,000	78,086	Complete
ATP:GTP ratio = 3:1, [NTP] = 360 μM, [NDP] = 20 μM							
$k_{dis\_eff} = 0.075$ s^{-1}	8	19	566	38,547	20,000	78,086	Initiation only
$k_{dis\_eff} = 0.047$ s^{-1}	14	28	505	92,914	20,000	78,086	Complete
$k_{dis\_eff} = 0.038$ s^{-1}	16	32	477	128,136	20,000	78,086	Complete
ATP:GTP ratio = 4:1, [NTP] = 450 μM, [NDP] = 20 μM							
$k_{dis\_eff} = 0.075$ s^{-1}	9	21	553	47,945	20,000	78,086	Initiation only
$k_{dis\_eff} = 0.045$ s^{-1}	15	30	486	114,890	20,000	78,086	Complete
$k_{dis\_eff} = 0.0$ $k_{dis\_eff} = 0.035$ s^{-1}	19	35	455	160,818	20,000	78,086	Complete
ftsZ84 recovery: $k_{ex1} = 3 \times 10^{-4}$ μM^{-1}s^{-1}, [NTP] = 270 μM, [NDP] = 20 μM, $k_{dis\_eff} = 0.075$ s^{-1}							
ftsZ84 overexpression:							
[FtsZ84] = 24 μM (200%)	24	41	415	247,715	20,000	78,086	Complete
[FtsZ84] = 36 μM (300%)	80	70	218	1,390,710	20,000	78,086	Complete
ZipA overexpression *ftsZ84*:							
$B = 1122$, $P_a = 0.072$, (200%)	7	24	897	39,085	11,944	46,633	Initiation only
$B = 1572$, $P_a = 0.101$, (300%)	6	27	1215	37,631	8,515	33,245	Complete

Table 2: Wild-type parameter values

Parameter	Wild-type value	Units	Reference
$[FtsZ]_{Total}$	12	μM	Surovtsev *et al.*, 2008 [8]
[GTP]	90	μM	Surovtsev *et al.*, 2008 [8]
[GDP]	10	μM	Surovtsev *et al.*, 2008 [8]
B	672	–	Rueda *et al.*, 2003 [23]
P_a	0.043	–	Rueda *et al.*, 2003; Surovtsev *et al.*, 2008 [8,23]
κ	0.2	μM	Haney *et al.*, 2001 [10]
i_{max}	150	–	Surovtsev *et al.*, 2008 [8]
k_{ex1}	0.01	$\mu M^{-1}s^{-1}$	Mukherjee *et al.*, 1993; Chen *et al.*, 2005; Surovtsev *et al.*, 2008 [8,52,53]
k_{ex2}	0.005	$\mu M^{-1}s^{-1}$	Mukherjee *et al.*, 1993; Chen *et al.*, 2005; Surovtsev *et al.*, 2008 [8,52,53]
k_{dim1}	4	$\mu M^{-1}s^{-1}$	Chen *et al.*, 2005; Surovtsev *et al.*, 2008 [8,53]
k_{dim2}	40	s^{-1}	Chen *et al.*, 2005; Surovtsev *et al.*, 2008 [8,53]
k_{el1}	4	$\mu M^{-1}s^{-1}$	Chen *et al.*, 2005; Surovtsev *et al.*, 2008 [8,53]
k_{el2}	0.4	s^{-1}	Chen *et al.*, 2005; Surovtsev *et al.*, 2008 [8,53]
k_{an}	4	$\mu M^{-1}s^{-1}$	Chen *et al.*, 2005; Surovtsev *et al.*, 2008 [8,53]
k_{dis}	0.075	s^{-1}	Romberg and Mitchison, 2004 [11]
k_{dif}	78	$\mu M^{-3}s^{-1}$	Culbertson *et al.*, 2002 [54]
k_{bind1}	0.142	$\mu M^{-1}s^{-1}$	Haney *et al.*, 2001; Stricker *et al.*, 2002 [10,12]
k_{bind2}	0.0284	s^{-1}	Haney *et al.*, 2001; Stricker *et al.*, 2002 [10,12]

FIGURE LEGENDS

Figure 1:

Schematic diagram of the CAM-FF model. (A) The cell is conceptually divided into three compartments: (1) the cell caps; (2) the midcell; and (3) the midcell membrane. FtsZ moves between the cell caps and the midcell regions by diffusion. Exchange between the midcell region and the midcell membrane occurs on the interaction of FtsZ with membrane anchor sites and subsequent polymerisation. (B) Using the notation of Surovtsev *et al.*, (2008), the chemical reactions in our model are: (i) nucleotide exchange; (ii) dimerization; (iii) elongation; (iv) annealing; and (v) polymer breakdown following GTP hydrolysis (i-iii are reversible, iv-v are assumed to be irreversible). (C) Depending on the anchor density, an FtsZ polymer may bind to one or more anchor sites. (D) The fraction of membrane-bound polymers expected to be attached by a single FtsZ-anchor interaction, as a function of polymer length for anchor density P_a = 0.043 and equilibrium constant κ = 0.2 μM. (E) Z-ring contraction pulls the membrane inwards against the outward force from the surface-tension generated at the inner membrane.

Figure 2:

The contraction threshold. The contraction threshold is shown as a function of ρ, the dimensionless ratio of the radius of the Z-ring to the original radius, *i.e.* contraction proceeds from ρ = 1 to ρ = 0. Parameter values are as follows: α = 20,000, r = 0.4 μm, ω = 0.1 μm.

Figure 3:

Drug targeting: GTP binding vs FtsZ polymerization. Decreasing the rate of FtsZ polymerisation is a more efficient approach to prevention of cell division than inhibition of GTP binding. The initiation (α) and completion (CT) thresholds are shown. All other parameter values are as shown in Table 2.

Figure 4:

Drug targeting: ZipA. Decreasing the number of ZipA binding sites available (solid line) is an effective approach to prevention of cell division. The initiation (α) and completion (CT) thresholds are shown (dashed lines). All other parameter values are as shown in Table 2.

Figure 5:

ATP binding and hydrolysis by the ftsZ84 temperature-sensitive mutant. Solid line: Wild-type solution. All other plots $k_{ex1} = 3 \times 10^{-4}$ μM^{-1}s^{-1}. Dotted line: 42ºC, $k_{dis\_eff} = 0.075$ s^{-1}. Dashed lines correspond to reduced temperatures. Short dash: A 2-fold decrease in the rate of ATP hydrolysis. Long dash: A 3-fold decrease in the rate of ATP hydrolysis. (A) ATP:GTP ratio 2:1, [NTP] = 270 μM, [NDP] = 20 μM. (B) ATP:GTP to 3:1, [NTP] = 360 μM, [NDP] = 20 μM. (C) ATP:GTP to 4:1, [NTP] = 450 μM, [NDP] = 20 μM. All other parameters as shown in Table 2.

FIGURES

Figure1:

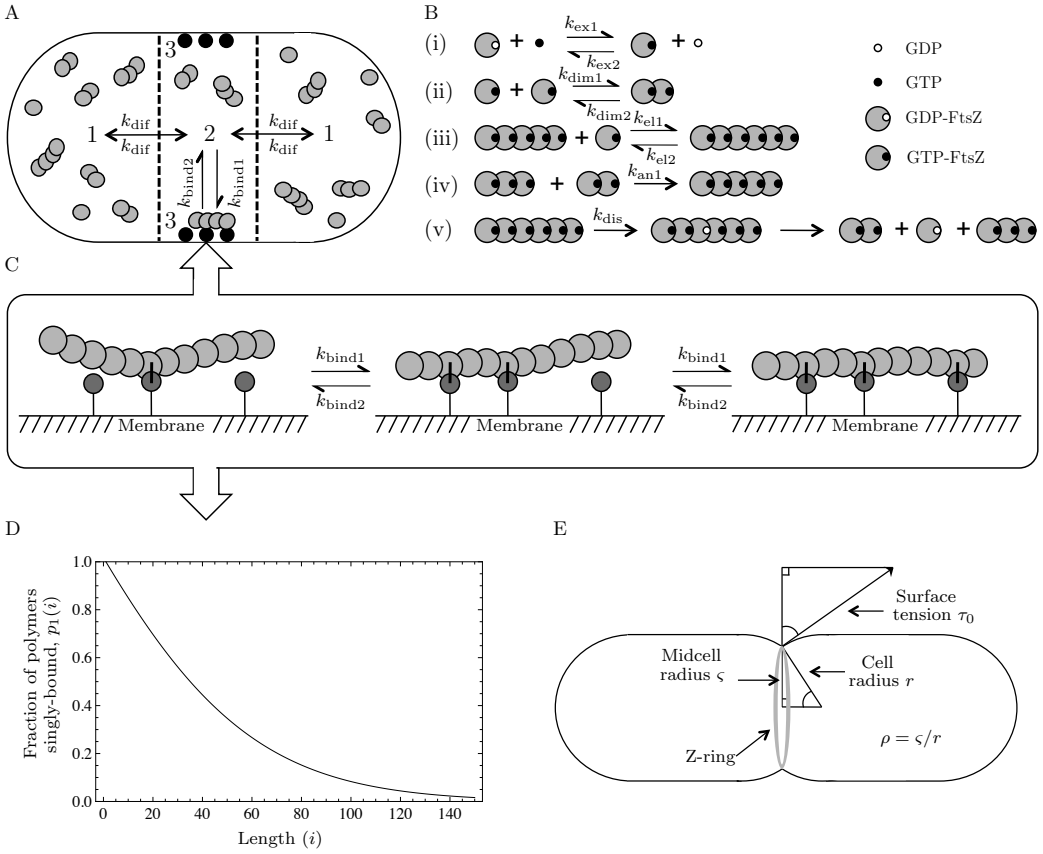

Figure2:

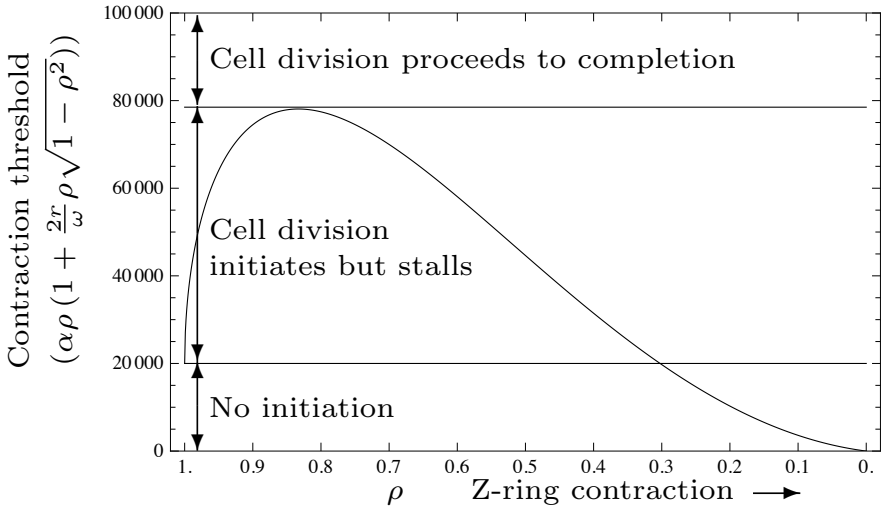

Figure3:

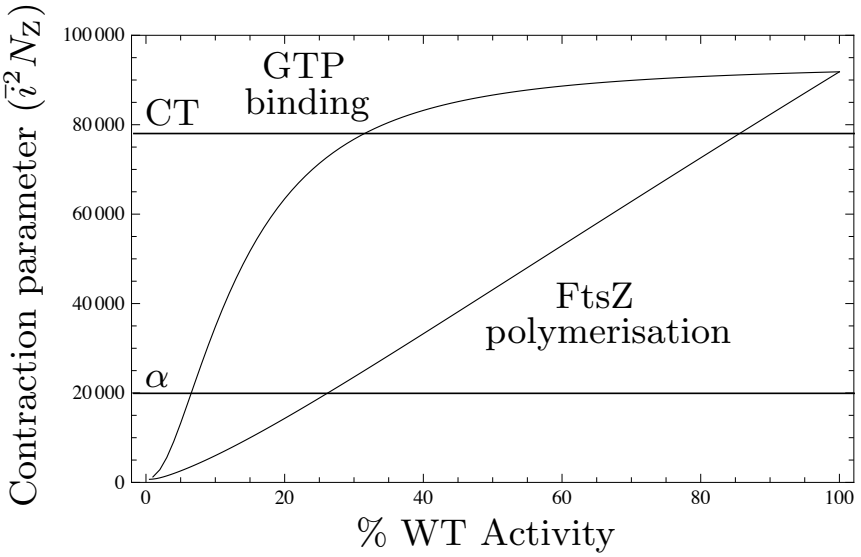

Figure4:

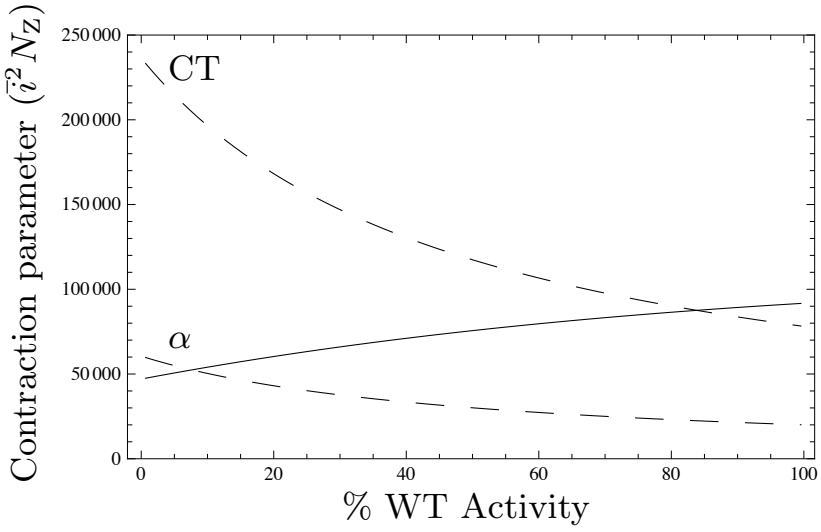

Figure5:

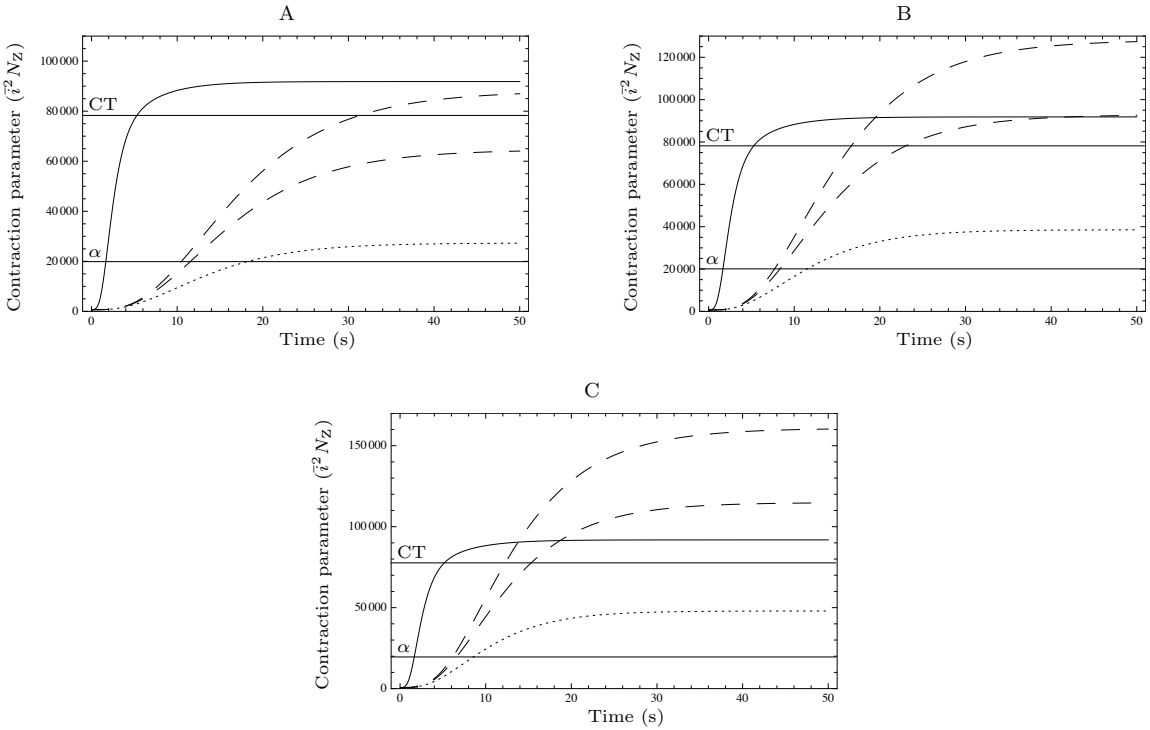

TOC GRAPHIC

For Table of Contents Only